American Journal of Applied Sciences 5 (11): 1580-1587, 2008
ISSN 1546-9239

Harmonics Phase Shifter for a Three-Phase System with Voltage Control by Integral-Cycle Triggering Mode of Thyristors

I. Badran, A.L. Mahmood and M.T. Lazim
Department of Electrical Engineering, Philadelphia University, Jordan

Abstract: In integral-cycle triggering mode of voltage control, subharmonic as well as higher order harmonic components are generated in the load voltage waveforms of a three-phase system. These harmonic components are found to be unbalanced in phase displacement. The correction of the unbalanced phase displacement angles of a particular subharmonic or higher order harmonic for this type of triggering is investigated to solve the limitation of use of this important type of control as a drive and many other industrial applications. In this research a new phase shifting technique is proposed to correct the unbalanced phase displacement angles in the three-phase system. This technique depends on shifting the waveforms of either phase B or phase C or both by multiples of 2π. A microprocessor-based harmonic phase shifter is designed and tested with three-phase resistive and induction motor loads. It is found that there is a well agreement between the theoretical and experimental results and it is believed that the major problem of harmonics phase unbalances associated with the integral-cycle triggering mode of thyristors when used with three-phase circuits have been solved in the present research.

Key words: Harmonics, integral cycle control, power electronics, phase angle correction, phase shifter, ac motor speed control

INTRODUCTION

Load voltage control by means of switching a pair of inverse parallel connected thyristors or triac is well established. It is customary to use modes of thyristor triggering known as integral-cycle triggering whereby burst of complete cycles of current are followed by complete cycles of extinction[1-4]. Integral-cycle triggering results in conduction patterns that contain subharmonics of the supply frequency and so constitute a form of step-down frequency changing that can be considered as a form of frequency changer. Also integral-cycle triggering results in a considerable reduction in the amplitudes of the higher order harmonics as compared with other triggering techniques and it is possible that Radio Frequency Interference (RFI) is negligible[2]. The phase-control switching can produce higher order harmonics and heavy inrush current while switching on in a cold start[5], while integral-cycle control circuits have the advantage of low inrush current due to zero voltage switching ease in construction and low hardware cost. Therefore, integral-cycle control loads have been widely used in resistive loads, such as heaters, oven, furnaces and spot welders[6-8]. Also it is used in speed control of single-phase induction motor[9] and dc series motor[10].

As a frequency changing scheme, integral-cycle triggering was found not feasible for applications in the three-phase systems exploiting this technique for ac motor speed control[11]. This is because the amplitudes and phase displacement angles of the higher order harmonic and subharmonic components of the integral-cycle controlled waveform are determined by the conduction period N and the control period T and the order of the individual harmonic. The three-phase analysis of voltage and current waveforms and phase relationships of the generated harmonic and subharmonic components for different circuit configurations are described in[12,13].

Consider a three-phase resistive load with line voltage control as shown in Fig. 1. The resulting three-load voltage waveforms are identical and so are the three-load current waveforms. The supply frequency components are found to be balanced, since they are 120^o apart in time-phase while the phase displacement angles of a particular subharmonic or higher order harmonic are unbalanced[11,12]. Due to the unbalanced phase relationships of the subharmonic components, these components represent a source of trouble when these voltage waveforms are used to feed ac machines for speed control purposes[11]. In this research an attempt is made to study the phase unbalanced

Corresponding Author: I. Badran, Department of Electrical Engineering, Philadelphia University, Jordan

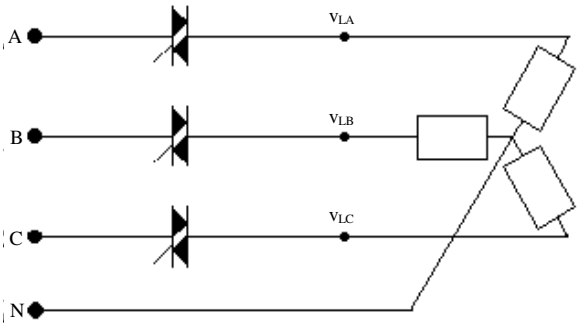

Fig. 1: Four-wire star-connected load with line controllers

characteristics of the subharmonics as well as the higher order harmonics generated due to integral-cycle triggering and to find a new phase shifting technique that is capable of correcting the unbalanced phases based on microprocessor implementation[14].

THE PROPOSED PHASE SHIFTING TECHNIQUE

Figure 2 shows the waveforms of the load voltages for the case when using integral-cycle control with control period T = 2 and conduction period N = 1, for the circuit shown in Fig. 1 with R-L load. Let the notation 1, 2, 3 denote the three phases A, B and C respectively. Thus the load voltage (v_{Lj}) for any j^{th} phase will have the general form[12].

$$v_{Lj} = \sqrt{2}\,V\sin\left(\omega Tt - \gamma_j\right) \quad \frac{\gamma_j}{T} \le \omega t \le \frac{2\pi N + \phi + \gamma_j}{T} \tag{1}$$

where

$$j = 1, 2, 3$$
$$\gamma_1 = 0, \quad \gamma_2 = 2\pi/3, \quad \gamma_3 = 4\pi/3$$
$$\phi = \tan^{-1}\frac{\omega L}{R}$$

Fourier analysis of Eq. 1 results in the following mathematical expressions:
for $n \neq T$, the dc component is:

$$a_0 = \frac{\sqrt{2}\,V}{\pi T}\left[1 - \cos\phi\right] \tag{2}$$

The amplitude c_n of n^{th} order subharmonic or higher order harmonic as well as its phase displacement ψ_n are found as follows:

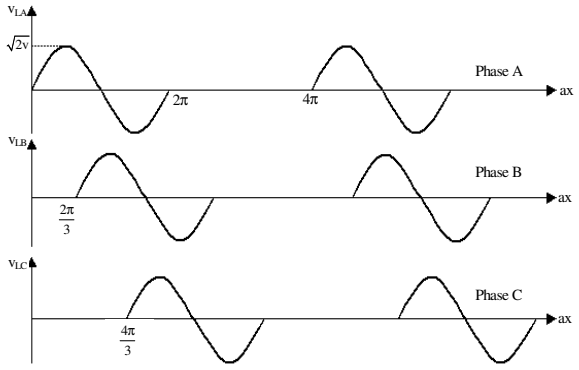

Fig. 2: Typical load voltages for phases A, B and C

$$a_{nj} = \frac{\sqrt{2}\,V}{\pi\left(T^2 - n^2\right)}\left[\begin{array}{l} T\left\{\cos\frac{n\gamma_j}{T} - \cos\phi\cos\frac{n}{T}\left(2\pi N + \phi + \gamma_j\right)\right\} \\ -n\sin\phi\sin\frac{n}{T}\left(2\pi + \phi + \gamma_j\right)\end{array}\right] \tag{3}$$

$$b_{nj} = \frac{\sqrt{2}\,V}{\pi\left(T^2 - n^2\right)}\left[\begin{array}{l} T\left\{\sin\frac{n\gamma_j}{T} - \cos\phi\sin\frac{n}{T}\left(2\pi N + \phi + \gamma_j\right)\right\} \\ +n\sin\phi\cos\frac{n}{T}\left(2\pi + \phi + \gamma_j\right)\end{array}\right] \tag{4}$$

$$c_{nj} = \sqrt{a_{nj}^{\ 2} + b_{nj}^{\ 2}}$$

$$c_{nj} = \frac{\sqrt{2}\,V}{\pi\left(T^2 - n^2\right)}\left[\begin{array}{l} T^2\left\{\cos\frac{n}{T}\left(2\pi N + \phi\right) - \cos\phi\right\}^2 \\ +\left\{T\sin\frac{n}{T}\left(2\pi N + \phi\right) - n\sin\phi\right\}^2\end{array}\right]^{1/2} \tag{5}$$

$$\psi_{nj} = \tan^{-1}\frac{a_{nj}}{b_{nj}}$$

$$\psi_{nj} = \tan^{-1}\frac{\left[\begin{array}{l} T\left\{\cos\frac{n\gamma_j}{T} - \cos\phi\cos\frac{n}{T}\left(2\pi N + \phi + \gamma_j\right)\right\} \\ -n\sin\phi\sin\frac{n}{T}\left(2\pi + \phi + \gamma_j\right)\end{array}\right]}{\left[\begin{array}{l} T\left\{\sin\frac{n\gamma_j}{T} - \cos\phi\sin\frac{n}{T}\left(2\pi N + \phi + \gamma_j\right)\right\} \\ +n\sin\phi\cos\frac{n}{T}\left(2\pi + \phi + \gamma_j\right)\end{array}\right]} \tag{6}$$

For n = T, the supply frequency component, the Fourier coefficients are:

$$a_{Tj} = \frac{\sqrt{2}\,V}{4\pi T}\left[\cos\gamma_j - 2(2\pi N+\phi)\sin\gamma_j - \cos(2\phi+\gamma_j)\right] \quad (7)$$

$$b_{Tj} = \frac{\sqrt{2}\,V}{4\pi T}\left[\sin\gamma_j + 2(2\pi N+\phi)\cos\gamma_j - \sin(2\phi+\gamma_j)\right] \quad (8)$$

$$c_{Tj} = \frac{\sqrt{2}\,V}{4\pi T}\left[2(1-\cos 2\phi) + 4(2\pi N+\phi)(2\pi N+\phi-\sin 2\phi)\right]^{1/2} \quad (9)$$

$$\psi_{nj} = \tan^{-1}\frac{a_{nj}}{b_{nj}} \quad (10)$$

It is found in[15] that the n^{th} frequency component of load current in phase A (ψ_{n1}) leads that of phase B (ψ_{n2}) by $120^o\frac{n}{T}$ and (ψ_{n2}) leads (ψ_{n3}) by $120^o\frac{n}{T}$ also. However, if the phase displacement of the j^{th} phase (γ_j) is shifted according to the following relationship:

$$\gamma_j = \gamma_j' + 2\pi m_j \quad (11)$$

where, γ_j represent the new shifting angle and

$$m_j = 1,2,...,T-1.\ m_1 = 0,\ \gamma_1' = 0,\ \gamma_2' = 2\pi/3,\ \text{and}\ \gamma_3' = 4\pi/3$$

This new value of γ_j do not affect the amplitude and phase angle relationships of the supply frequency components at the load voltages. It can be seen from Eq. 5, that the amplitude of the n^{th} harmonic is independent of γ_j, which means that, the variation of γ_j does not affect the harmonic amplitude spectrum of the j^{th} phase. Only the phase displacement angle ψ_n of the n^{th} harmonic is changed as could be seen from Eq. 6. The phase displacement angle ψ_{nj} of the n^{th} harmonic varies with the variation of m_j.

Now after shifting the load voltage waveform of phase B or C or both of them by multiple of 2π the n^{th} frequency component of load current in phase A (ψ_{n1}) leads that of phase B (ψ_{n2}) by

$$(120^O + 360^O \times m_2)\frac{n}{T} \quad (12)$$

and (ψ_{n1}) leads (ψ_{n3}) by:

$$(240^O + 360^O \times m_3)\frac{n}{T} \quad (13)$$

The harmonic amplitude spectrum and the phase angle relationships for the load voltage waveforms of Fig. 2 are shown in Fig. 3 and 4 respectively. It is seen that, the phase displacement angles of the subharmonics and the higher order harmonics are unbalanced. Now, if the phase displacement angle of phase B, i.e., ψ_{n2} is shifted by 180° then the phase displacement angles of the 1st harmonic (25 Hz) and the 5th harmonic (125 Hz), as for example, become balanced.

The new values of ψ_{n2} for the 1st, 3rd and 5th harmonics which are $\psi_{12} = 210^o$, $\psi_{32} = 270°$ and $\psi_{52} = 150^o$ respectively give the value $m_2 = 1$ and the new value of γ_2 is equal to 480^o. The harmonic amplitude spectrum and the phase displacement angles of the supply frequency component remains unchanged with the new value of γ_2, while the phase displacement angles of the 1st, 3rd and 5th harmonics changed as shown in Fig. 5a, c and d respectively. It is found that this shifting technique makes the phase displacement angles of the n^{th} harmonic order balanced (120° between the phases) except when n is a multiple of 3 where in this case the phase displacement angles become in phase for all values of N and T except when T is a multiple of 3. Also it is noticed that the phase shifting of the phase displacement angles used in this technique do not depend on the value of N. This means that, the values of γ_2 and γ_3 that makes n^{th} order harmonic balanced for certain values of N and T can make it balanced as well for the same value of T with N = N-1, N-2, …, 1. Table 1 shows the values of m_2

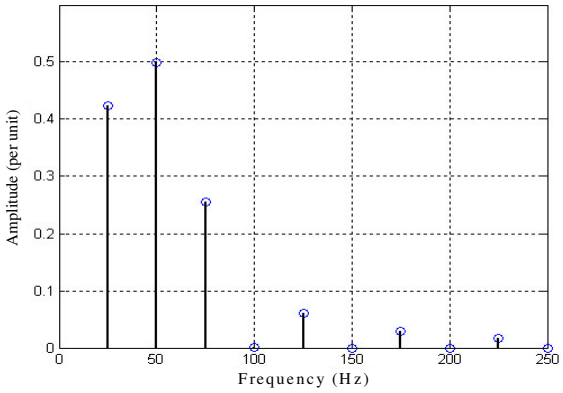

Fig. 3: Harmonic amplitude spectrum for T = 2 and N = 1, R-load

Table 1: The phase displacement angles for typical values of T and N

T	N	m_2	m_3
2	1	1	0
4	3-1	1	2
5	4-1	3	1
7	6-1	2	4
8	7-1	5	2
10	9-1	3	6

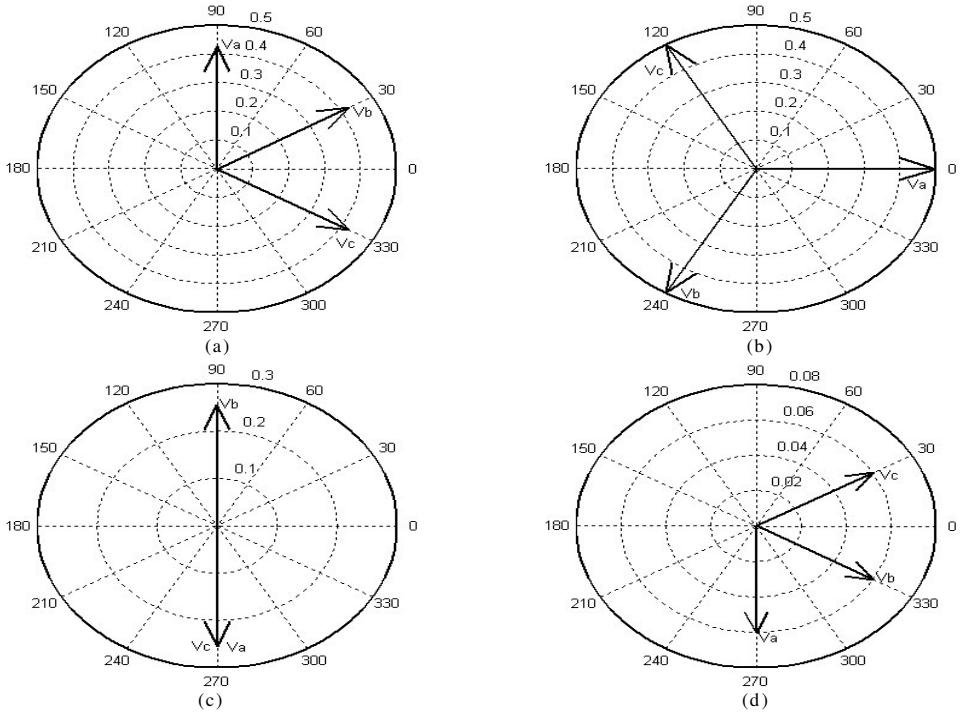

Fig. 4: Phase displacement angles for T = 2 and N = 1, R-load (a): Phase displacement angles for the 1st harmonic (25 Hz) (b): Phase displacement angles for the supply frequency component (c): Phase displacement angles for the 3rd harmonic (75 Hz) (d): Phase displacement angles for the 5th harmonic (125 Hz)

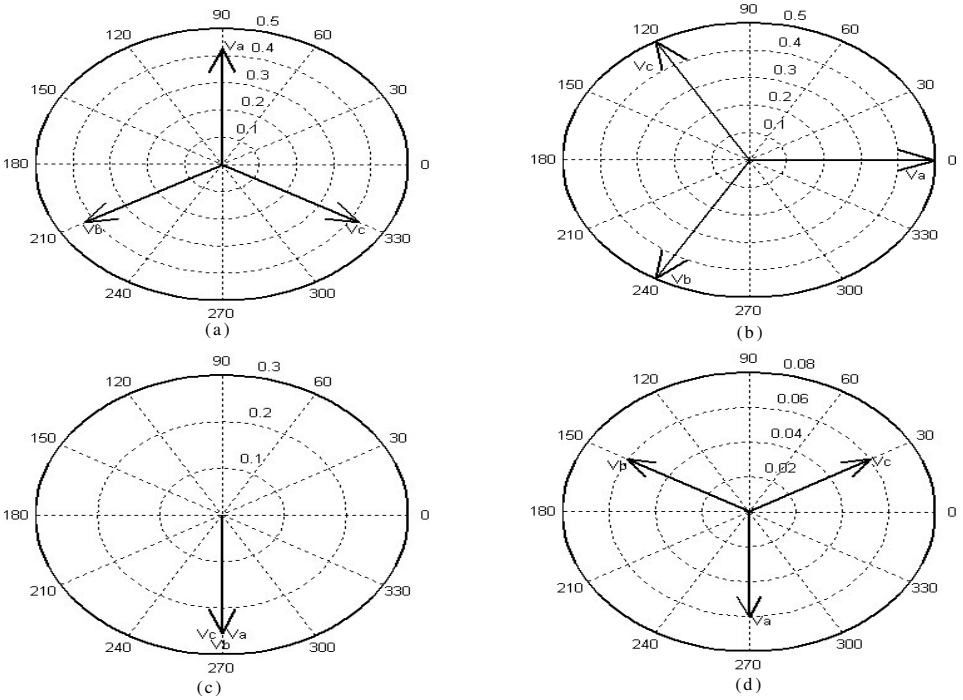

Fig. 5: Phase displacement angles for (a): 1st harmonic (25Hz) (b): supply frequency component (50Hz) (c): 3rd harmonic (75Hz) (d): 5th harmonic (125Hz)

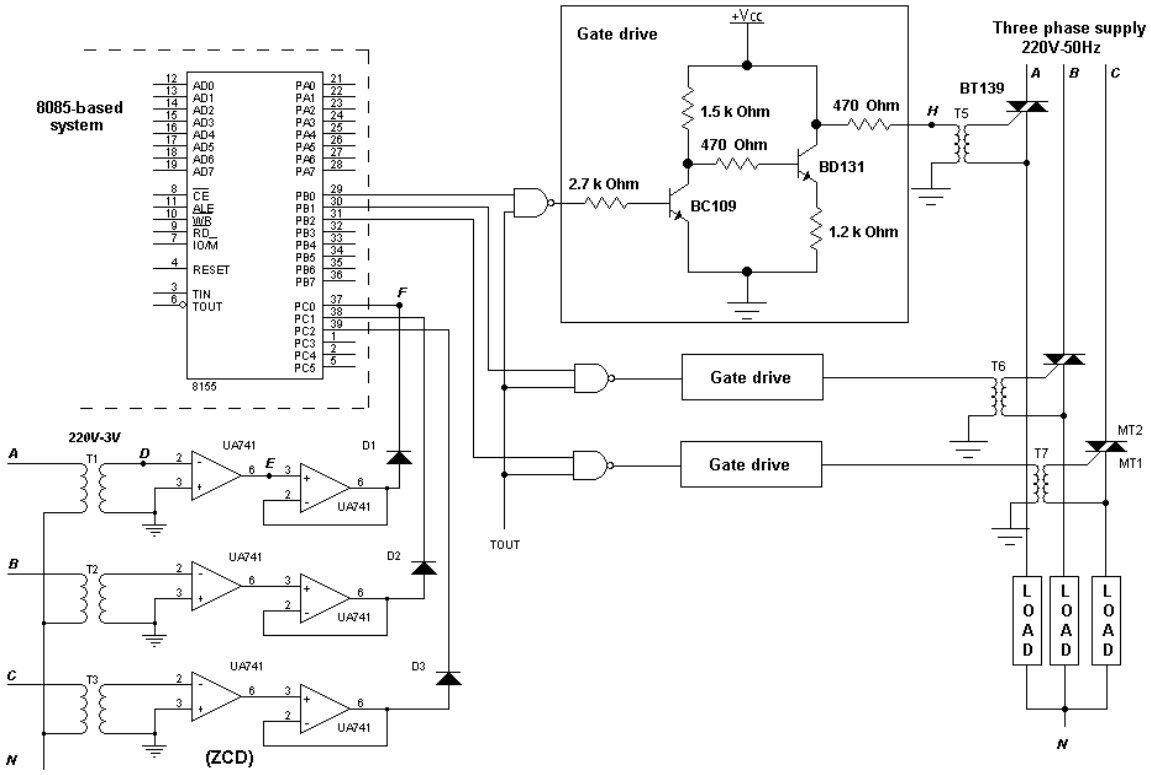

Fig. 6: Schematic circuit diagram

and m_3 which make the phase displacement angles of the n^{th} harmonic either balanced or in phase for typical values of T and N. This technique cannot correct the phase displacement angles of a particular subharmonic or higher order harmonic if T is a multiple of 3.

PRACTICAL IMPLEMENTATION

The schematic diagram of the microprocessor-based harmonic phase shifter for integral-cycle control is shown in Fig. 6. After reducing the three-phase supply voltage by the step-down transformers (T_1, T_2 and T_3), the Zero Crossing Detector (ZCD) circuits produces the 180° pulses to an 8085 microprocessor-based system. The microprocessor now can sense the zero-instant of the ac supply. Then the conduction of the triacs started by sending high pulses to the gate drive circuits (the gate drive circuit used from[16]). The output of each gate drive circuit is connected to pulse transformers (T_4, T_5 and T_6), that are used to isolate the microprocessor circuit from the power circuit. In order to ensure successful triggering of the triac the trigger voltage must be maintained for the entire conduction period. This can be achieved by using a square pulses at high frequency and these pulses are generated by the

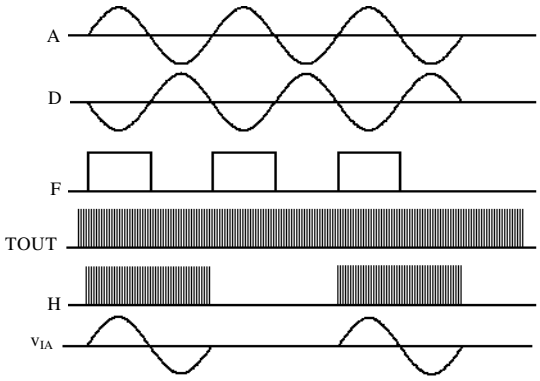

Fig. 7: Waveforms of signals at different points in the control circuit

timing circuit. A NAND gate is used to modulate the higher frequency pulses with the main conduction pulse.

Figure 7 shows the signals at different stages in the control circuit for phase A programmed for a conduction period of 1 cycle out of two. The square pulse E goes through a buffer circuit that is found necessary for the elimination of the dc bias generated in the comparator. The microprocessor sends a square

pulses through PB0 of the 8155 with ON/OFF ratio equal to N/(T-N).

EXPERIMENTAL RESULTS

The control circuit shown in Fig. 6 was built and tested in the laboratory with a three-phase balanced resistive load. Fig. 8 and 9 show oscillograms of the load voltage waveforms v_{LA}, v_{LB} and v_{LC} for the case when T = 4 and N = 2 before and after the application of the phase-shifting technique respectively. It is obvious that the phase-shifting procedure does not affect the wave shapes of the load voltage or current.

The system was tested also with a three-phase, cage-type induction motor described in Appendix A. The stator windings were connected in 4-wire, star-connected form. Practically this type of voltage control, i.e. integral-cycle, is found to produce some problems to the motor such as noise, vibration and heat rising to the motor windings. These problems become severe especially at high voltages and when the motor runs continuously. However, Table 2 shows the speed measurement of the motor n_s at different values of N and T using a digital tachometer before and after the phase displacement angles correction in addition with the frequency of rotation for each case that is calculated using the following equation of the three-phase induction motor speed[17]:

$$n_s = 120\frac{f}{p} \quad (14)$$

where, p = number of poles and f = supply frequency.

It is important to mention that the motor rotates in the reverse direction for some cases after the correction of the phase displacement angles and this is due to the variation in the phase sequence after the correction of the phase displacement angles.

However, the above results show that, the motor speed n_s is changed after the correction of the phase displacement angles. This is because the phase displacement angles of the first harmonic become balanced, i.e. separated by 120^o in time phase and it will produce its own speed. This means that after the correction of the phase displacement angles of the first harmonic, the motor began to rotate at the desired subharmonic frequency.

The three-phase induction motor is loaded by a dc dynamometer available in the laboratory to examine the performance of the motor under load condition. The dc

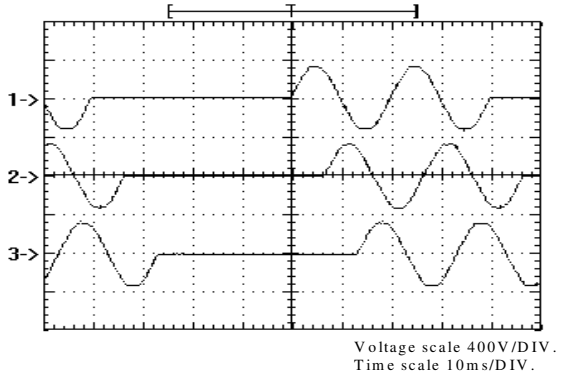

Fig. 8: Load voltage waveforms of phases A, B, C respectively before the correction of the phase displacement angles

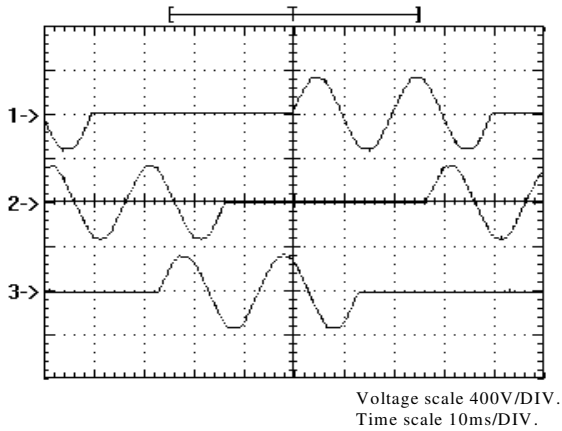

Fig. 9: Load voltage waveforms of phases A, B, c respectively after the correction kof the phase displacement angles

Table 2 : The speed measurement of motor n_s at different values using phase-shifting technique and friqunecy of rotation of each sace

T	N	n_s (r.p.m.) before using shifting technique	Frequency of rotation (Hz) (Experimental)	n_s (r.p.m.) after using shifting technique	Frequency of rotation (Hz) (Experimental)	Frequency of the 1st harmonic (Hz) (Theoretical)
4	2	1914	31.9	760	12.6	12.5
4	3	2922	48.7	1006	16.8	12.5
5	2	2190	36.5	605	10.1	10
7	3	2455	40.9	480	8	7.1
7	4	2893	48.2	546	9.1	7.1
8	3	2534	42.2	369	6.15	6.2

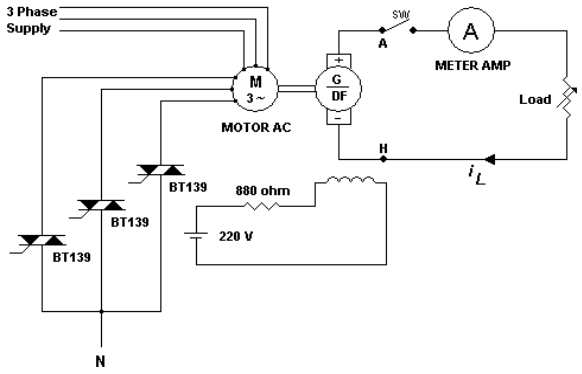

Fig. 10: Connection diagram for separately-excited de dynamometer

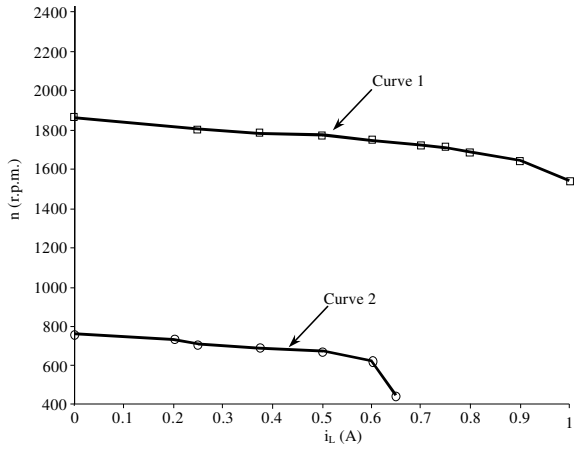

Fig. 11: Speed-current characteristic

dynamometer is connected as a separately excited machine as shown in Fig. 10. The specifications of the 3-phase motor and the dynamometer are given in Appendix B. The field winding of the dynamometer is connected to a 220V dc source and the field current is set to the maximum permissible value. The motor speed n_s is then measured at different values of load current (i_L) for T = 4 and N = 2 for both before and after correction cases of ψ_{nj}, the results are shown on curve1 and curve 2 in Fig. 11 respectively. It is found that, the motor speed is reduced after the correction of ψ_{nj} and this is obvious since the motor rotates at the 1st harmonic frequency. The highest value of the load current shown on curve2 is less than that on curve1, this is because the generated e.m.f. in the dynamometer proportional to motor speed n_s and any reduction in the speed leads to further reduction in the generated e.m.f. which in turn reduces the load current. Also any reduction in the value of the load resistance R in order to increase the load current at a certain value of V_{AH} leads to a reduction in the speed. This limitation in the loading machine performance does not allow us to take further readings to reach maximum loading of the motor.

CONCLUSION

The unbalanced sets of subharmonic and higher order harmonic voltages generated by integral cycle control technique create severe problems for ac machines as they found to cause excessive heat, mechanical vibrations and noise. Therefore, this type of control was abanded as an ac motor speed controller since many years ago. The proposed phase shifting technique in the present work is a try to solve the inherent limitation of this important type of control by shifting the second and third phases of the three-phase system by multiples of 2π. This technique is found to be more suitable than using the phase-angle control scheme to correct the unbalanced phase displacement angles of the generated harmonics. The last scheme is found to cause unbalanced harmonic amplitude spectrums for the three phases. It is found, from the theoretical and practical tests, that the performance of the three-phase induction motor with phase corrected voltage waveforms is very similar to that when fed from balanced sinusoidal voltages of the same amplitude and frequency when using the proposed phase-shifter. Finally, it is believed that the major problems associated with integral-cycle triggering control technique, when used for speed control of ac motor, have been solved in the present work.

ACKNOWLEDGMENTS

The authors wish to acknowledge the support and encouragements given by Ass. Prof. Xavier Kestelyn and all the staff of the L2EP laboratory in ENSAM school of engineering in Lille City -France.

REFERENCES

1. Gallagher, P.J., A.B. Barret and W. Shepherd, 1970. Analysis of single-phase rectified thyristor controlled load with integral-cycle triggering. Proc. Inst. Elec. Eng., 117 (2) 409-414.
2. Lingard, B.W., R.W. Johnson and W. Shepherd, 1970. Analysis of thyristor controlled single-phase loads with integral-cycle triggering. Proc. Inst. Elec. Eng., 117 (2): 607-608.
3. Gallagher, P.J. and W. Shepherd, 1975. Operation of two parallel connected thyristor controlled resistive loads with integral-cycle triggering. IEEE Trans. Ind. Electron. Control Instrumentation, IECI-22 (4): 510-515.

4. Shepherd, W., 1975. Thyristor Control of ac Circuits. Bradford University Press, England.
5. Syed Jamil Asgher, M., 1999. fine power control by discontinuous phase-controlled switching. IEEE Trans. Circuits Syst., 46 (3): 402-405.
6. Chun Li, J.A.M. and J.A.M. Wilsun Xu, 2001. On the ambiguity of defining and measuring inter-harmonics. IEEE Power Eng. Rev., pp: 56-57.
7. Mohan, N., T. Undeland and W. Robbins, 1995. Power electronics. 2nd Edn. New York: Wiley.
8. Krein, P., 1998. Elements of power electronics. New York: Oxford Univ. Press.
9. Krishnan, R., B. Ilango, S. Selvarary and S. Gunasekaran, 1980. Single-phase induction motor speed control with integral-cycle switching. IEEE Trans. Ind. Electron. Control Instrumentation, IECI-27 (4): 308-311.
10. Fetih, N.H., G.M. Abdel-Raheem and G.A. Girgis, 1988. Speed control of a DC series motor using an integral-cycle controlled single traic. IEEE Trans. Energy Conversion, 3 (3): 618-623.
11. Lazim, M.T. and W. Shepherd, 1985. Analysis of induction motor subjected to nonsinusoidal voltages containing subharmonics. IEEE Trans. Ind. Appli., IA-21 (4): 956-965.
12. Lazim, M.T. and W. Shepherd, 1982. Three-phase circuits with voltage control by integral-cycle single-phase mode triggering of thyristors. IEEE Trans. Ind. Appli., 46 (5): 507-520.
13. Lazim, M.T., 1981. Modulation techniques in the speed control of electric motors. Ph.D. Thesis, University of Bradford, England.
14. Mahmod, A.L., 2001. Microprocessor-based phase shifter for integral-cycle control. M.Sc. Thesis, Al-Nahrain University, Iraq.
15. Yong Nong Chang, Gerald Thomas Heydt and Yazhou Liu, 2003. The Impact of switching strategies on power quality for integral cycle controllers. IEEE Trans. Power Delivery, 18 (3): 1073-1078.
16. Arifur Rahman, Syed Enamul Haque and Ibrahim Abdul Rahman AL-Gadhi, 1980. A digital self-compensating method for integral-cycle power control of rl loads. IEEE Trans. Ind. Electron. Control Instrumentation, IECI-27 (2): 49-53.
17. Nasar, S.A. and L.E. Unnewehr, 1979. Electromechanics and Electric Machines. John Wiley and Sons, Inc.